Final Report

Federal Agency	DOE
FOA Name	Co-Optimization of Fuels and Engines
FOA Number	DE-FOA-0001461
Nature of Report	Final Report
Award Number	DE-EE0007981 / 0003; 1505-VTO
Award Type	Grant
Prime Recipient	Louisiana State University Attn: Winona Ward Louisiana State University and A&M College Sponsored Programs 202 Himes Hall Baton Rouge LA 708030100 Business Point of Contact: Dana R. Tuminello dimpson@lsu.edu 225-578-1076 Technical Contact: Ingmar Schoegl ischoegl@lsu.edu 225-578-4332
Prime Recipient Type	University
Project Title	Micro-Liter Fuel Characterization and Property Prediction
Principal Investigators:	Ingmar Schoegl (PI), LSU Shyam Menon (co-PI), LSU Eric Petersen (co-PI), TAMU Tianfeng Lu (co-PI), UConn
Prime Recipient DUNS Number	075050765
Date of Report	June 10th, 2022
Period Covered	Mar. 1, 2017 – Feb. 28, 2022

LSU

Final Report - DE-EE0007981

Ingmar Schoegl (PI)

Micro-Liter Fuel Characterization and Property Prediction

1. Project Introduction

The DOE Co-Optima initiative seeks to accelerate the introduction of affordable, scalable, and sustainable high performance fuels for use in high-efficiency, low emission engines. Co-optimized fuels and engines offer the opportunity to build on long-term research in both fuels and engines, where advances over the last ten years have identified combustion engine strategies that - especially if optimized to run on new fuels - would offer higher gas mileage and produce less engine-out pollutants than current engines.

The project "Microliter Fuel Characterization and Property Prediction" addresses DOE's stated interest in enabling small volume (<20 µl), high throughput (>100 tests/device/month) measurements of transportation fuels and blends that are relevant to co-optimized fuels and engines. In this context, the ability to quantify the performance of a fuel in terms of autoignition metrics (e.g. octane number/sensitivity), combustion properties (e.g. flame speed) and physical properties (e.g. volatility and viscosity) is of significant interest. Predictions of fuel performance in a combustion engine require a link to be made between small volume measurements and combustion behavior of a fuel blend at engine relevant conditions.

2. Objectives

The project seeks to establish a foundation for small volume high throughput fuel testing, where relevant fuel metrics are quantified in a micro combustion experiment.

- Quantify combustion metrics of transportation fuels (e.g. octane number, flame speed)
- Construct an experimental prototype that can operate at elevated pressures
- Develop prediction models linking small volume measurements to engine relevant conditions
- Demonstrate small volume / high throughput testing capabilities in blind tests

3. Approach

Approach as Originally Proposed

The approach for micro-liter fuel characterization relies on cyclical combustion events within a heated micro-tube. This combustion mode is known as FREI (Flames with Repetitive Extinction and Ignition) and relies on self-excited instabilities that are sensitive to fuel properties. A total sample volume of 20 ml is stored on a disposable microfluidic chip, dispensed via a MEMS droplet generator, and mixed with air to create desired stoichiometry and mass flow rate. Within the micro-tube, a temperature profile (300-1400K) is established by external heating, whereas the desired operating pressure (25-50 bar) is regulated by a pressure controller downstream of the micro-tube. The time required to capture individual data points lies in the order of 10-20 seconds, which allows for high throughput testing. FREI characteristics are evaluated for sweeps of mass flow rates and pressure. Image analysis provides information on ignition, extinction and flame propagation, which have been shown to be sensitive to fuel octane numbers.

The overall approach aligns with Sub-Topic 5 of the original FOA, i.e. "Small volume, high throughput fuel testing". The main objective is to demonstrate the feasibility of micro-liter fuel characterization as a method with smaller sample volumes and higher throughput than conventional approaches (Schoegl/LSU). A broadened scope includes engine-relevant physical fuel metrics (Menon/LSU) and thus

encompasses Sub-Topic 1 ("Fuel characterization and fuel property prediction"). Small-volume testing requires microfluidic fuel delivery and sensing (Gartia/LSU). It further needs to be validated against data from established experimental methods (Petersen/TAMU), whereas numerical analyses require reduced kinetic models (Lu/UConn).

Adjustments

Early results from a piezo-electric droplet generator (Menon/LSU) illustrated oscillatory behavior of ejected droplets, where characteristics are a strong function of surface tension and viscosity, both of which were targeted physical properties. At the same time, work on microfluidic chips (Gartia/LSU) faced challenges as a key manufacturing facility was only intermittently accessible. As a majority of anticipated microfluidic property measurements could be obtained from droplet observations, work on microfluidic chips was abandoned, while droplet work was refocused on physical property measurements.

Challenges Encountered

Combustion experiments rely on post-processing of image data, where high-dynamic-range (HDR) imaging was used to capture flame chemiluminescence data as well as black-body emission from a silicon carbide filament used for pyrometric thermometry. Camera sensor noise was found to be a limiting factor to high accuracy measurements, which necessitated the development of suitable compensation models.

Dissemination of Results

At the time of writing, results were documented and disseminated in 17 archival journal publications and 16 conference papers. Unpublished data are expected to result in several additional publications.

4. Project Timeline and Structure

The project started on March 1st 2017, and was initially scheduled to conclude on February 29th, 2020. A first no-cost extension was requested to account for initial delays due to procurement and design of critical component. LSU laboratories shut down due to Covid-19 on March 16th 2020; experimental work partially resumed mid June, with full access to laboratories restored on August 24th, 2020. Unavoidable delays led to a second no-cost extension, with a final project end date of February 28th, 2022.

The project combines four components that are documented as follows:

A. Micro-Combustion (I. Schoegl, PI / LSU)
B. Physical Droplet Measurements (S. Menon, co-PI / LSU)
C. Reference Measurements (E. Petersen, co-PI / TAMU)
D. Mechanism Reduction (T. Lu, co-PI /UCONN)

5. Results

Key Accomplishments

- Confirmed existence of essential combustion modes up to 25 bars, which doubles peak pressure of comparable experiments documented in published work
- Documented the loss of an unstable combustion regime at diluted conditions, creating a new pathway for fuel testing at high pressures and prediction of octane rating
- Established framework for non-contact temperature measurements and machine-learning based classification of combustion regimes
- Demonstrated feasibility of piezo-electric fuel delivery and pathway for droplet-based measurements for surface tension, viscosity, vapor pressure and heat of vaporization
- Obtained high quality shock tube data for DOE reference blendstocks
- Contributed reduced mechanisms for combustion simulations

A. Micro-Combustion (PI: I. Schoegl)

Summary

Within the project, the objective of reaching engine-relevant pressures was reached in two steps: (i) an intermediate pressure setup using components rated at 150 psig was used for 1-10 bar tests, and (ii) a high pressure setup using components rated for 500 psig was used in tests up to 25 bar. Substantial efforts were made in the areas of custom instrumentation (pyrometry and camera calibration) as well as analytic predictive modelling of combustion phenomena and post-processing of measurement data. The project was successful in verifying that combustion experiments are sensitive to both octane rating and octane sensitivity. Dilution of the air/fuel mixture with nitrogen was highly effective in preventing flashback at high pressures. All three combustion phenomena that are commonly found in micro-channel experiments – weak flames, flames with repetitive extinction and ignition (FREI), and normal flames that occur at low, intermediate and high flow velocities, respectively – were observed at all tested pressures. Experiments conducted at 25 bar represent the highest documented pressure in a comparable experimental setup. Further, a direct transition from weak flames to normal flames was documented for the first time. It was demonstrated that this transition point is sensitive to the octane rating, where a newly developed machine-learning model was used to assist in the classification of flame regimes.

i. Intermediate Pressure Experiment (1-10bar)

During the initial phase of the project, test pressures were limited to 4 bar. A change of approach in pressure regulation allowed for tests at 1-10 bar (limited by pressure limits of standard components).

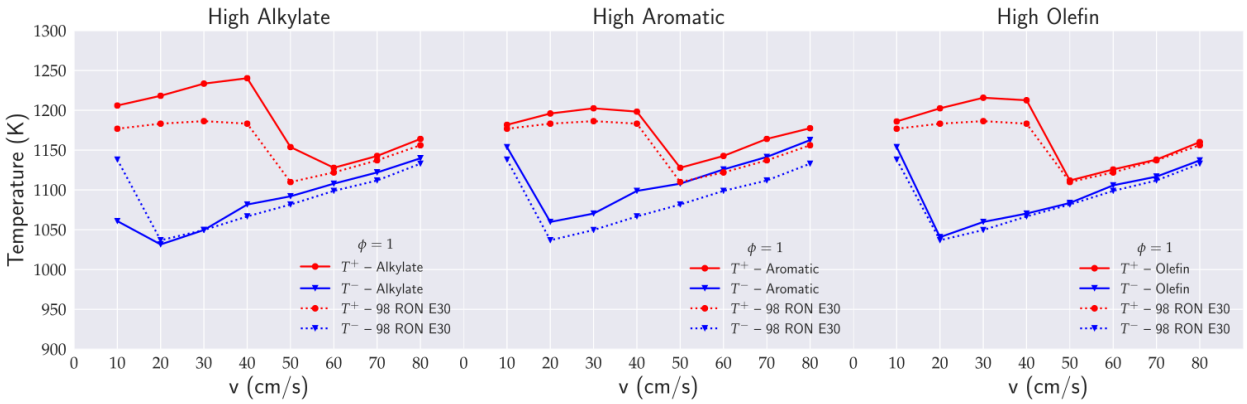

Figure 1. Microcombustion results for CoOptima fuel blends with matched RON and partially matched Octane sensitivity S. Fuel samples courtesy of Szybist/ORNL. Results presented at 2018 AMR (I. Schoegl/LSU)

Octane Sensitivity. Tests in the initial phase of the project were limited to the 4 bars (FY2018). Nevertheless, tests with CoOptima fuel blends provided by Szybist/ORNL provided evidence that microcombustion experiments are capable of differentiating between fuels with different Octane sensitivity (S). Figure 1 compares the performance of three CoOptima fuels to 98 RON E30: all fuels share a 98 RON, while S of the high alcylate fuel is significantly lower (S≈1.2 vs. S≈10.6). Similar to findings by ORNL, fuels with matched RON and S show comparable combustion characteristics, whereas a deviation in S impacts results. Figure 1 does, however, also indicate that high accuracy temperature measurements are essential. Measurements used a newly implemented pyrometry technique, where a need for improved algorithms and associated uncertainty quantification was evident (measurement uncertainties were estimated at ±20-30 K).

Effects of Dilution and Pressure. After an update of the main pressure controller, the intermediate pressure setup was operational over the targeted 1-10 bar range in FY2019. Experimental tests involved the impact of dilution and pressure on combustion of ethane/air mixtures, where an expected tendency for flashback with increasing pressure was confirmed. Flashback was successfully prevented by reducing O2 levels from 21% to 12%. All three relevant combustion phenomena were documented for 10 bar in a 1mm tube. Associated flow velocities were about approximately 80% lower than at atmospheric pressure, i.e. no detrimental effect preventing small sample testing was found, as corresponding overall mass flow rates do not vary significantly. Testing did, however, reveal non-negligible effects of thermal gas/wall interactions.

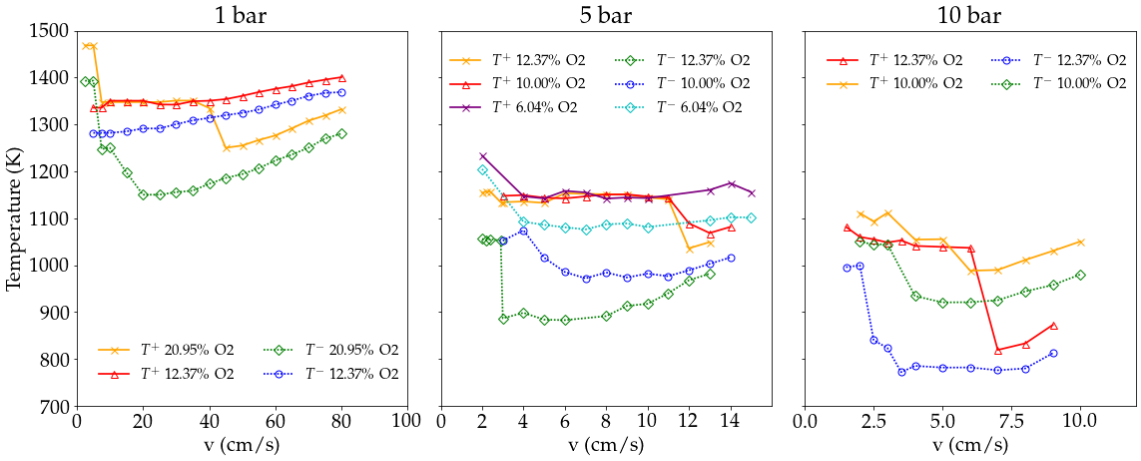

Figure 2: Results for pressure and dilution effects (Roohani, Sauer and Schoegl, PROCI 2020).

Figure 2 shows results that document pressure and dilution effects that are inherent to the experiment (Roohani, Sauer, and Schoegl, PROCI 2021). The results are novel in multiple ways: (i) at 10 bar peak pressure, the LSU setup exceeded pressures of most comparable experiments; (ii) measurements involve a thin filament pyrometry approach that had not been previously used in comparable setups. The pyrometry technique developed at LSU involves high dynamic range (HDR) imaging with conventional machine vision cameras. Notably, the low temperature limit of 800K significantly improves upon comparable work with conventional cameras that are typically used for substantially higher temperatures. Most importantly, (iii) the results show, – for the first time, – the loss of an intermediate unstable combustion regime due to dilution effects. In addition to experimental data, the study also employed an analytical predictive model (see Section 5.A.iii).

Sensitivity to Octane Rating. In FY2020, the combustion behavior of mixtures of primary reference fuels (PRF)and air was evaluated experimentally for multiple dilution and pressure conditions. Experiments were carried out in an externally heated microchannel with 1 mm inner diameter, where a syringe pump was used for delivery of liquid fuels. Flame characteristics were investigated for 1, 5, and 10 bar over a range of dilution levels using N2 as the diluent. Tests focused on the quantification of extinction and ignition temperatures and the differentiation of transitions between the three different flame modes. The temperature profile along the micro-channel was again estimated via the LSU thin filament pyrometry technique (TFP), which uses a silicon carbide (SiC) fiber placed adjacent to the channel wall. Extinction and ignition temperatures are evaluated by correlating axial positions of flame edges to the temperature profile. Similar to the earlier study, it was found that increasing dilution raises the extinction temperature. Most importantly, results showed clear evidence of the impact of octane rating on experimental results. Figure 3 shows data obtained at 5 bar for various dilution levels and three PRF's. Blue shading marks

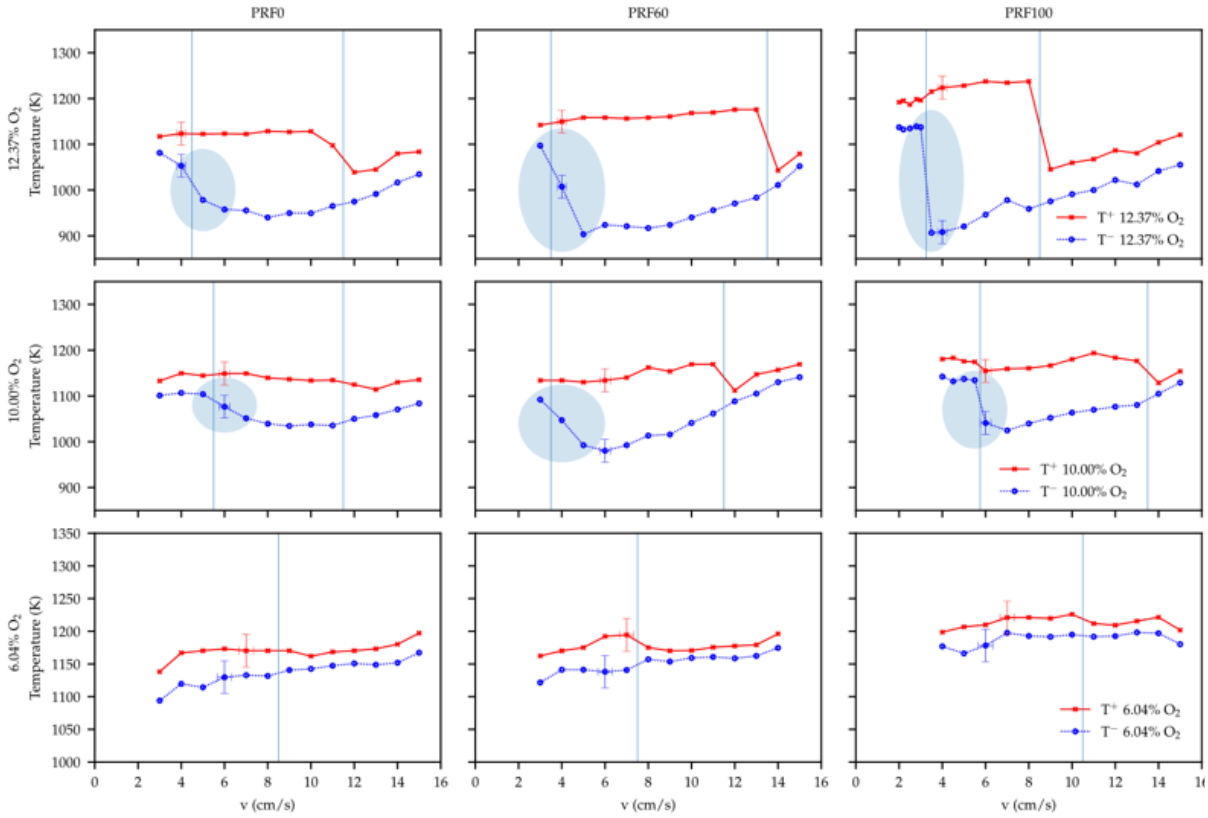

Figure 3: Results for effect of dilution (12.37/10/6.04% 02 – top to bottom) and octane rating (PRF0/60/100 – left to right) at 5 bar (Roohani, Sauer and Schoegl, USNCM 2021).

regions where a transition from stationary weak flames to transient FREI occurs. For n-heptane (PRF0), the transition is gradual, whereas for isooctane there is a sharp demarcation. This effect is attributed to the impact of low temperature chemistry that causes premature extinction of flames traveling into low temperature regions during FREI. Figure 3 further illustrates that at the lowest temperature, the intermediate FREI regime is lost, and a direct transition from weak to normal flames occurs. A schematic illustrating differences of flame topology is shown in Figure 4, where weak flames with low luminescence transition to well defined, bright normal flames. In undiluted (or slightly diluted) mixtures, three regimes are observed, whereas in (highly) diluted mixtures, the FREI regime contracts to a single transition.

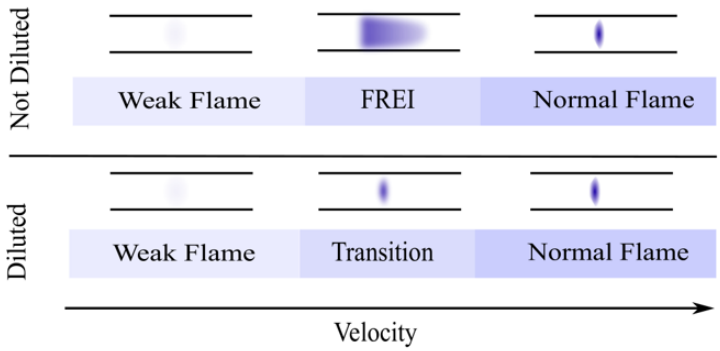

Figure 4: Transitions between combustion regimes (Roohani, Sauer and Schoegl, ASME POWER 2021).

Close inspection of results further reveals that transition velocities between flame regimes are sensitive to the octane number (ON). Figure 5 illustrates postprocessed data for experiments conducted at 10 bar, where direct transitions from weak to normal flames are observed. Data clearly illustrate that the transition velocity is a strong function of ON and thus is an indirect metric suitable for octane prediction.

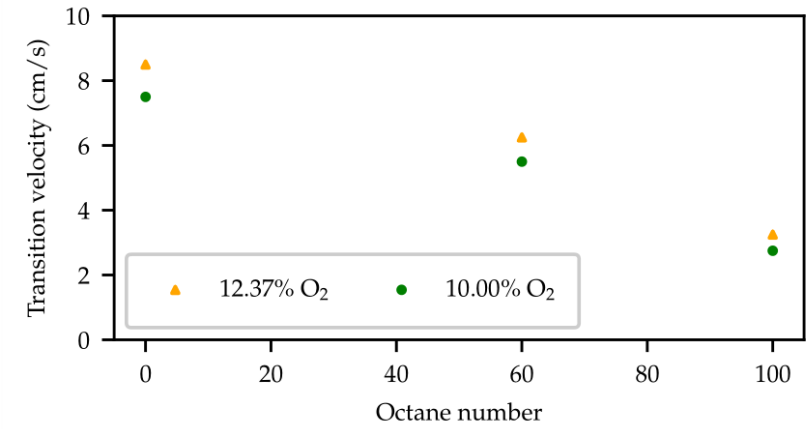

Figure 5. Transition velocity from the weak flame regime for different octane numbers at 10 bar.

Although the transition between different flame regimes can be identified by inspection, a machine-learning (ML) algorithm was developed to assist with the identification of transitions based on flame image data. The ML model involves an artificial neural network that is detailed in Section 5.A.iv.

ii. High Pressure Setup

The high pressure setup was assembled from components rated up to 500 psig, and used redesigned manifolds that incorporate a filament positioning mechanism. Leaks of O-ring seals required a partial redesign of the manifolds; leaks were resolved by FY2021, which allowed for pressurized tests as detailed below. The redesign also targeted the use of a thinner 14um diameter SiC filament, which increases the accuracy of pyrometry measurements while also addressing difficulties in procurement of the 56um diameter filament used in earlier work. While initial issues with the filament positioning mechanism were addressed, the thinner SiC filament showed a tendency to break during the mounting process, which was not fully resolved at the time of writing.

In order to address fundamental questions about existence and dynamics of pertinent flame regimes at elevated pressures, tests were conducted without pyrometry, where results include location and extent of observable combustion zones. Although no temperature data are available, this approach still allows for a detection of transition velocities between flame regimes. An initial cross-validation with ethane/air mixtures from the intermediate pressure setup (Roohani, Sauer, and Schoegl, PROCI 2021) yielded comparable results, which confirmed that initial leaking issues were fully addressed. In subsequent tests, the pressure was first increased to 15 and 20 bar for ethane/air mixtures. Both pressures exceed the highest documented pressure of 12 bar in published work for comparable experiments (Kikui et al, PROCI 2015). Initial experimental data obtained for diluted ethane/air mixtures used a mass flow controller for gaseous mixtures, which was a viable approach up to 20 bars. In order to demonstrate higher pressures, the fuel supply was switched to methane, where tests were conducted up to 25 bars, at which point the calibration of the mass flow controllers started to become unreliable. Representative data for diluted ethane/air and methane/air mixtures are presented in Figures 6 and 7, respectively.

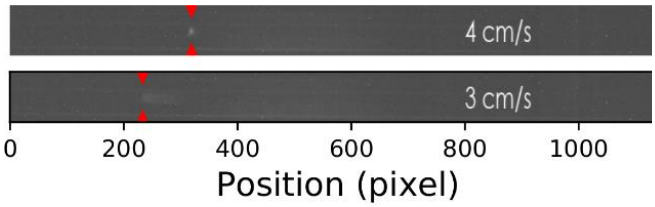

(a) 20 bar / 12.37% O_2.

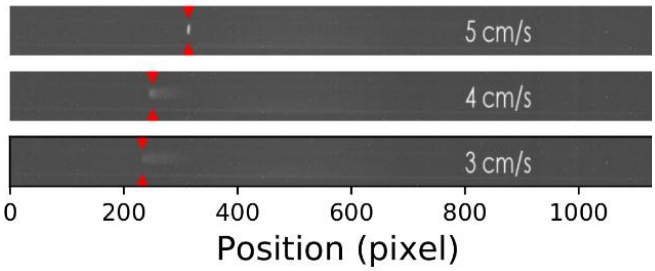

(b) 20 bar / 10% O_2.

Figure 6. Combustion of diluted C2H6/air at 20 bar (Akinpelu and Schoegl, ASME POWER 2021).

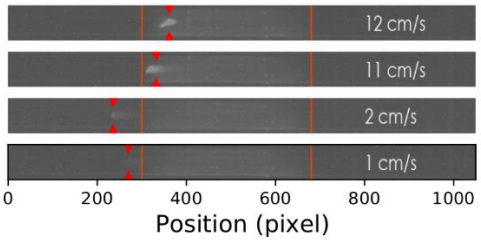

(a) 25 bar / 12.37 % O_2.

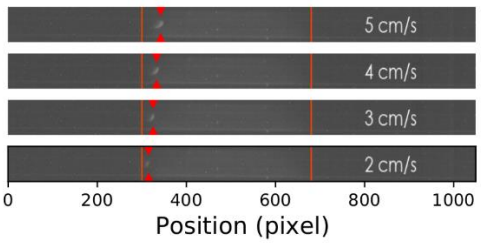

(b) 25 bar / 6.04 % O_2.

Figure 7. Combustion of diluted CH4/air at 25 bar (Akinpelu and Schoegl, USNCM 2021)

Figures 6a and 6b illustrate transitions from stable 'normal' flames at the highest velocity to the cyclical FREI regime at lower velocities. The significance of these results is that it was possible to demonstrate for the first time that these combustion regimes exist at high pressure, which was previously assumed but had not been verified in experiments. Images shown in Figure 7a show 3-dimensional flame behavior at the highest velocities that were most pronounced at the highest tested pressure. At the lower oxygen concentration, results remained inconclusive due to the low chemiluminescence signal inherent to CH4 combustion, where long exposure times result in insufficient signal-to-noise ratio. Subsequent work focused on the installation of a filament for pyrometry.

iii. Qualitative Prediction Model

During the initial phase of the project, substantial efforts were directed towards the development of a simple theoretical model to predict combustion behavior of the micro-tube experiment. This model was developed as a predictive tool to assist in constraining the parameter space for tests at elevated pressure. The newly developed model successfully predicts quenching behavior, transitions between combustion regimes, and temperature levels for normal (strong) flames. The model is qualitative by nature, and captures the coupling between heat transfer effects and first order chemical kinetics via large activation energy asymptotics. Due to this simplification, the model has inherent limitations in predicting weak flame and ignition phenomena; however, the model provides valuable guidance for scaling up pressure, where predictions are consistent with observations. Most significantly, the qualitative analysis provides insights for the loss of FREI at high dilution based on classical S-curves. Results were published in Schoegl, Sauer, and Sharma, *Combust. Flame* 2019 and used for Roohani, Sauer, and Schoegl, *PROCI* 2021.

iv. Neural Network for Flame Classification

As detailed in Section 5.A.i, transitions between combustion regimes were identified as markers of fuel-specific combustion behavior. Within each flame regime, noticeable differences exist in both shape and luminosity where transition points can be used to obtain insights into fuel characteristics. While transitions from weak flame to FREI and FREI to normal flame as easily identified, the elimination of FREI at high dilution levels complicates the identification of transition points from weak flames to strong flames as illustrated in Figure 4.

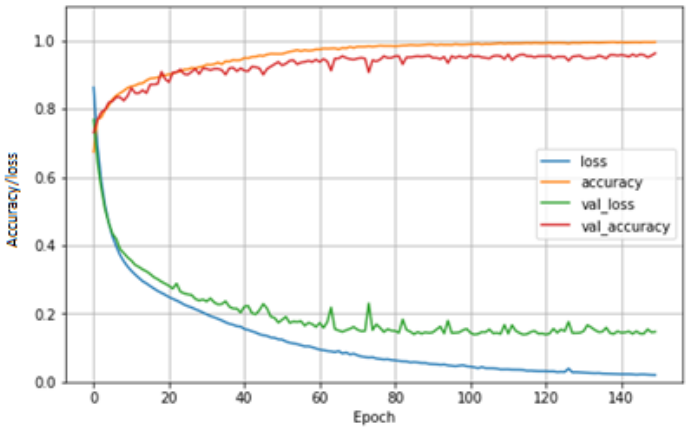

Figure 8. Accuracy of flame classification (Roohani, Sauer, Schoegl, ASME POWER 2021).

In order to facilitate data analysis, an artificial neural network was implemented to classify flame types and detect transitions in absence of FREI. Flame images are obtained from a monochrome camera equipped with a 430 nm bandpass filter to capture the chemiluminescence signal emitted by the flame. Sequences of conventional flame photographs are taken during the experiment, which are computationally merged to generate high dynamic range (HDR) images. A convolutional neural network (CNN) is introduced to classify the flame regime. The accuracy of the model is calculated to be 99.5, 99.32, and 99.5% for the "training", "developing", and "testing" dataset, respectively. This level of accuracy is achieved by conducting a grid search to acquire optimized parameters for CNN. Furthermore, a data augmentation technique based on different experimental scenarios is used to generate flame images to increase the size of the dataset. Figure 8 presents training and developing set accuracy and loss for each "epoch", which are equivalent to iterations in numerical simulations.

v. Uncertainty Quantification of High Dynamic Range Pyrometry.

Non-contact temperature measurements via thin filament pyrometry (TFP) follow an approach that has originally been developed for high temperature applications, and is based on photographic images of the filament obtained at multiple wavelengths. The project requires the capability of reaching relatively low temperatures for a small diameter (10-75 micro meter) silicon carbide filament. One of the stated targets

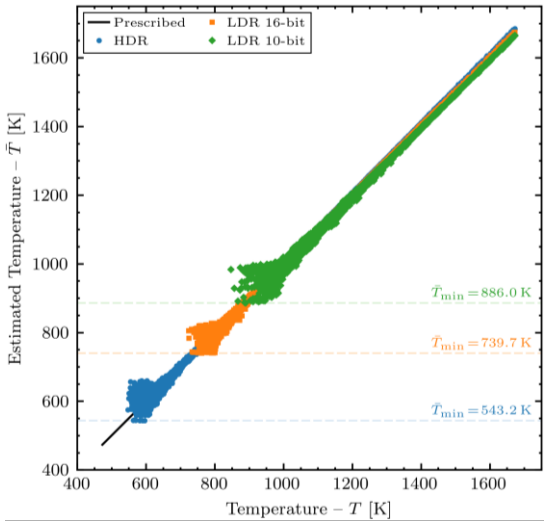

Figure 9. Uncertainty quantification for pyrometry measurements (Sauer and Schoegl, *Measurement* 2019)

of the project was to measure temperatures with high confidence, where a preferred outcome was single-digit uncertainty at observed temperature levels (650-1400K). An initial implementation achieved a low temperature limit of 850K, with an uncertainty estimated at ±20-30K, which was deemed insufficient, and an improved algorithm was implemented. As experimental validations of measurements are themselves susceptible to uncertainty in benchmark data, a simulation-based approach was chosen for an uncertainty quantification. Work in FY2018 focused on the image-processing portion, where the emission of radiation, image acquisition by a sensor with inherent noise characteristics, was simulated, and resulting synthetic images were processed with the updated pyrometry algorithm. Figure 9 shows results, where known and reconstructed temperatures are plotted on horizontal and vertical axes, respectively, i.e. ideal results follow the diagonal. The color coding compares the reconstructed temperature range of a conventional 10-bit camera sensor (green), a high bit count 16-bit sensor (orange), and the high dynamic range (HDR) approach pursued in this project (blue), where the latter combines multiple images with different exposure times. While all tests share the same high temperature limit, HDR clearly outperforms conventional low dynamic range (LDR) approaches. It is noted that while the lowest reconstructed temperatures were around 540K, the low temperature region is affected by sensor noise. Above 650K, confidence intervals were evaluated as smaller than 10K, meeting project requirements.

vi. Other Efforts

Camera Sensor Calibration. The objective of this effort is a compensation of sensor noise, which affects image quality especially at long exposure times. A successful reduction is essential for postprocessing of data with low signal-to noise ratio, which is of importance for both detection of weak flames as well as pyrometry at the temperature close to the lowest detectable values. The effort is ongoing and will be applied to post-process unpublished data.

Chemical Explosive Mode Analysis (CEMA). During the last year of the project, efforts targeted computational diagnostics of simulation data to obtain insights into processes that represent determining factors for ignition in the transient FREI mode, as well as the transition from weak flames to FREI, i.e. factors that were shown to correlate well with the fuel octane number. While preliminary results were presented at a regional conference, a final publication is expected after the conclusion of the project.

Publication List

See References 1-3 and 17-26 in Section 7.

B. Physical Droplet Measurements (co-PI S. Menon/LSU)

Summary

Observation of oscillation decay in droplets ejected by a piezoelectric droplet generator were shown to be an effective approach in determining physical properties such as viscosity and surface tension for emerging biofuels using μl quantities. Further, fuel evaporation characteristics yield information on vapor pressure and heat of vaporization. Specifications of the fuel delivery system are compatible with liquid fuel delivery requirements of the combustion experiment.

Nano-liter Fuel Delivery at Elevated Pressures.

Micro-combustion tests for fuels of interest to CoOptima involve limited (20µL) sample size, where it is necessary to supply metered quantities of liquid fuel at nano-liter per second (µL/min) flow rates. While a micro syringe based delivery system for low vapor pressure fuels was used for fuel delivery in combustion experiments, a less limiting approach involves the piezoelectric generation of a high frequency droplet train. The approach provides additional insights into physical fuel properties that are based on droplet metrics. The delivery system produces fine droplets, which vaporize, mix with air and

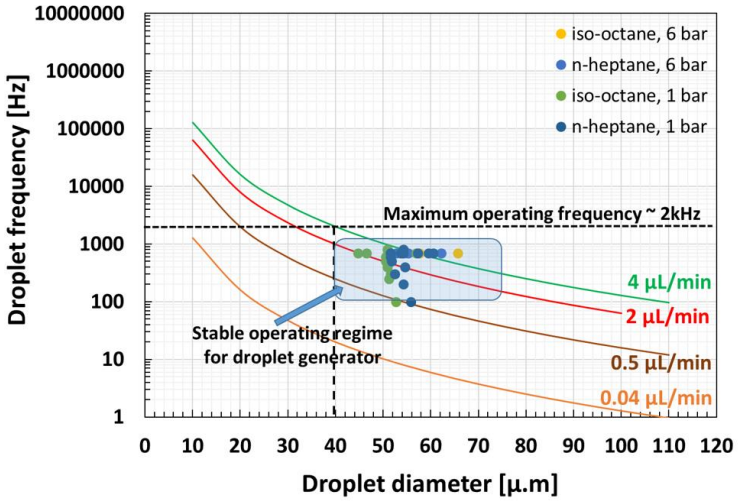

Figure 10. Operating conditions tested for nanoliter fuel delivery at ambient and elevated pressures (S. Menon/LSU)

provide a gaseous fuel-air mixture of desired stoichiometry to the micro-combustor, where engine-relevant pressure capabilities are critical to the success of the project.

A commercial off-the-shelf piezoelectric droplet generator was implemented as a micro-liter fuel delivery device. The ability to control droplet size in a range of 20-70 µm while independently varying fuel flow rate through adjustment of the operating frequency (1-1200 Hz) creates flow rates required for the micro-combustor setup (0.5-4 µL/min). Experiments conducted in FY2018 aimed at an assessment of the viability of the fuel delivery concept at elevated pressure. In parametric studies, the response of droplet size and velocity to input signal parameters was studied for high vapor pressure fuels at room temperatures (323 K) by implementing the setup in a chamber with controlled pressure and temperature. Figure 10 illustrates the operational range of the liquid fuel delivery system at ambient and elevated pressure levels, where markers represent tested conditions. Characteristics were evaluated up to 6 bar (87 psig), where elevated pressures reduced droplet velocity, but did not interfere with the overall performance of the system.

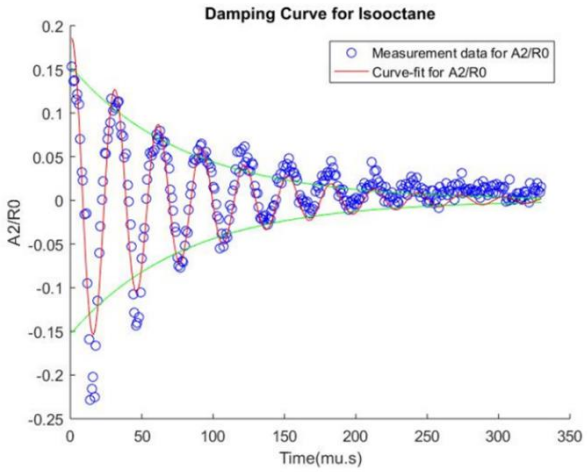

Figure 11. Sample damping curve for iso-octane. Data are used for physical property measurements, e.g. viscosity and surface tension (Dang, Zhao, Schoegl and Menon, *Meas. Sci. Technology* 2020).

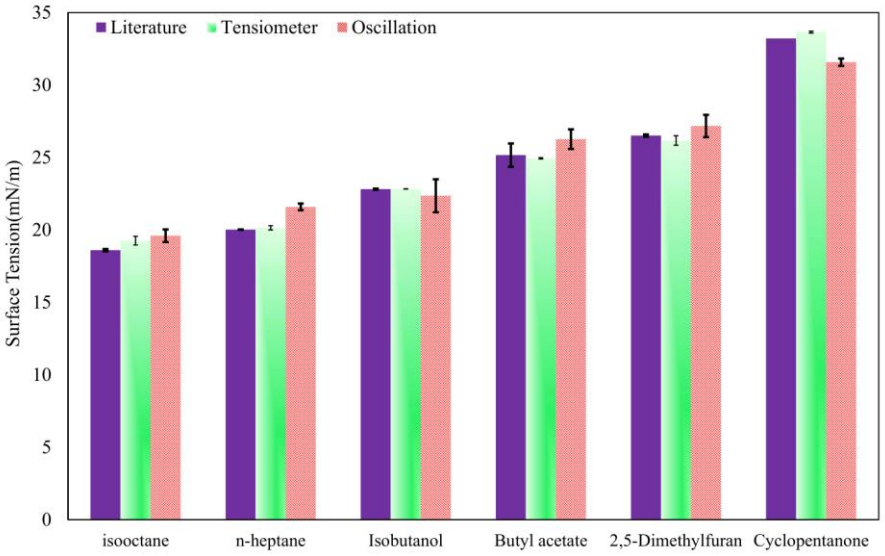

Figure 12. Results for surface tension (Dang, Zhao, Schoegl and Menon, *Meas. Sci. Technology* 2020).

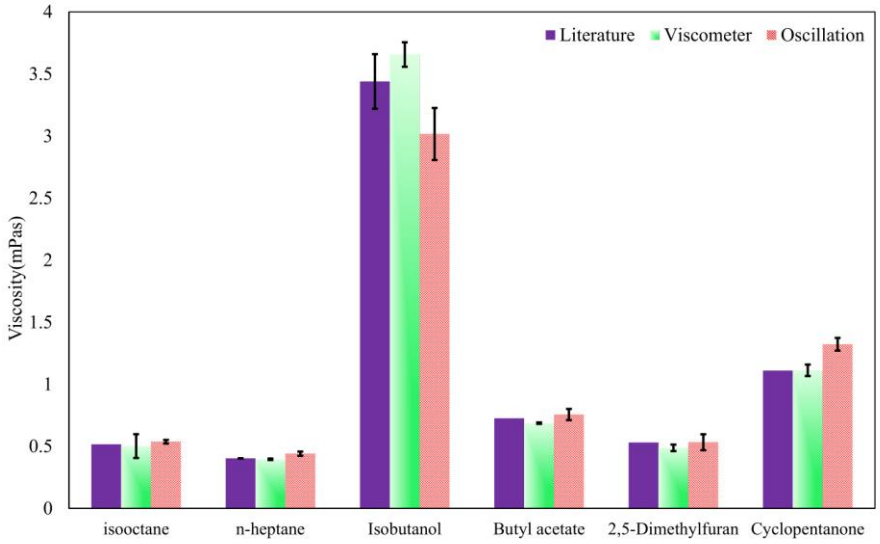

Figure 13. Results for viscosity measurements (Dang, Zhao, Schoegl and Menon, *Meas. Sci. Technology* 2020).

Surface Tension and Viscosity

Work on physical property prediction started with measurements of surface tension and viscosity using micro-liter quantities of fuel at atmospheric pressure, which were completed for several relevant fuels. Experiments were conducted that use high-resolution strobed imaging of moving fuel droplets to capture shape oscillation decay through image processing and analysis. Studied fuels include PRF's (iso-octane and n-heptane) as well as functional group molecules representative of biofuels including ketones, esters, alcohols, and furans from the Tier II selection of Co-Optima fuels. Measurement of surface tension and viscosity involve the observation of droplet dynamics post-injection from a piezoelectric droplet generator, where oscillations extracted from stroboscopic measurements are illustrated in Figure 11.

Tests were conducted to determine optimal strobe operation time for imaging the droplets as well as to find the best edge-tracking algorithm for droplet shape detection.

Figures 12 and 13 present measurement data for surface tension and viscosity, respectively. Droplet oscillation measurement results showed a maximum of 7% deviation in surface tension and 13% deviation in viscosity from literature data. The uncertainty in surface tension measurement through droplet oscillation ranges from 1–5% while that in viscosity ranges from 3–12%. The repeatability of the droplet oscillation process was confirmed through direct imaging. Measurement results for the current set of fuels utilized an average of 5 µL per fuel and required about 20 s per sample for data collection. In comparison, standard tensiometers and viscometers require about 15 ml and 7 ml of fuel sample respectively, and require about 2-3 minutes of operation each, to generate surface tension and viscosity measurements. Overall, the measurements show that the droplet oscillation dynamics based technique using a piezoelectric droplet generator provides a small-volume and high-throughput fuel screening technique.

Impact of Temperature on Measurements

Initial work was extended to assess effects of higher temperatures typical for fuel injection conditions in internal combustion engines. Two fuels were investigated, iso-butanol and a primary reference fuel (PRF 84), which is a mixture of isooctane and n-heptane. Surface tension and viscosity calculated at four different temperatures ranging from 30°C-55°C using the frequency and decay time associated with the fundamental mode are found to be within ~10% of reference values obtained from the literature. Complementary numerical simulations are performed that utilize a volume-of-fluid approach to track transient droplet oscillation along with heat and mass transfer in a 2D axisymmetric domain. Simulations, where droplet size and temperature can be independently varied, captured an expected decrease in oscillation frequency and increase in decay time, with increase in fuel temperature. The simulations were further used to study the relative contribution to deviations in surface tension and viscosity predictions due to heat and mass transfer from the droplet, as well as viscous effects violating the inviscid flow assumption in the droplet oscillation theory. Mass loss effects were found to be negligible. Temperature change due to heat transfer was found to have the next highest sensitivity, particularly for the more volatile PRF 84, which has a lower viscosity and associated Ohnesorge number. For isobutanol, which has a higher viscosity and Ohnesorge number, viscous effects contribute the most to deviation in fuel property predictions.

Heat of Vaporization

The final part of work on the piezo-electric droplet generator involved a droplet evaporation-based approach to predict heat of vaporization, vapor pressure, diffusion coefficient, and Lennard–Jones parameters for an unknown fuel. The approach uses droplet evaporation experiments conducted in a temperature and pressure controlled chamber to obtain a droplet evaporation slope (diameter vs. time). Multiple values of the slope would be obtained from multiple data sets for the same fuel. Correlation to fuel physical properties using the Abramzon-Sirignano model are used to back-calculate the vapor pressure and then obtain the heat of vaporization using the Clausius-Clapeyron equation.

The approach was further enhanced by assessing estimation schemes based on a combination of experiments and numerical simulations. Two schemes considering the isothermal evaporation of a moving droplet in ambient air were proposed, which combine droplet velocity and temperature measurements with some known properties to predict unknown properties in an iterative fashion. A baseline scheme, which only requires droplet size change measurements, was evaluated using test data for three liquid

Fuel	Temperature	HOV			Vapor pressure		
		Predicted	Reference	Deviation	Predicted	Reference	Deviation
n-heptane	18	3.40E5 ± 0.5E5	3.74E5	9.1	2.78E3 ± 0.9E3	2.41E3	15.4
	40	3.90E5 ± 0.4E5	3.67E5	6.4	3.86E3 ± 0.7E3	4.6E3	16
	60	3.70E5 ± 0.1E5	3.63E5	2.1	6.51E3 ± 0.1E3	6.84E3	4.9
	75	3.64E5 ± 0.4E5	3.60E5	1.1	8.44E3 ± 1.2E3	8.71E3	3.1
PRF 84	18	3.43E5 ± 0.2E5	3.28E5	4.7	2.04E3 ± 0.4E3	2.60E3	21.7
	40	3.39E5 ± 0.2E5	3.23E5	5.3	4.13E3 ± 0.5E3	4.88E3	15.3
	60	3.25E5 ± 0.5E5	3.18E5	2.2	6.83E3 ± 1.4E3	7.34E3	6.9
isobutanol	36	6.76E5 ± 0.6E5	6.90E5	2.0	1.39E3 ± 0.3E3	1.44E3	3.0
	60	6.73E5 ± 0.5E5	6.74E5	0.1	3.02E3 ± 0.4E3	3.18E3	5.0
	°C	J/kg		%	kPa		%

Table 1. Results for HOV and Vapor pressure estimations from droplet experiments (Dang, Gurunadhan, Ard, Schoegl, and Menon, *Int. J. Thermophysics* 2021).

fuels, comprising of alkanes and alcohols, as obtained in a temperature-controlled chamber. Results yielded temperature-dependent heat of vaporization and vapor pressure predictions within 10 % and 22 % of reference values, respectively (Table 1). An advanced scheme, which would require droplet temperature measurements, was evaluated numerically. The advanced scheme holds promise to improve prediction quality significantly, with deviations less than 2 % and 1 % for heat of vaporization and vapor pressure, while also predicting diffusion coefficient and Lennard–Jones parameters within 5 % and 8 %, respectively. It is expected that the combined set of approaches, which primarily track droplet evaporation, can be incorporated into a small-volume, high-throughput fuel screening process.

Publication List

See References 4-6 and 28-30 in Section 7 (as reported by co-PI).

C. Reference Measurements (co-PI E. Petersen/TAMU)

Summary

Work on reference measurements at Texas A&M involved shock tube measurements and flame speed measurements. For the former, work covered methanol, ethanol, isopropanol and a 4-component gasoline surrogate. Flamespeed measurements targeted blends of the 4-component surrogate and ethanol. In all cases, results were compared to simulations with kinetic mechanisms, e.g. Aramco 2.0 or the LLNL CoOptima mechanism.

Shock Tube Measurements

Methanol Kinetics. Ignition delay times of methanol-air mixtures, with Ar as diluent, were studied between 940 and 1540 K in a heated shock tube, for pressures up to 14.9 atm and for equivalence ratios of 0.5, 1.0, and 2.0. Water profiles were measured by utilizing a laser absorption technique in the 1350-to-1600-K temperature range, at an average pressure of 1.3 atm and for similar equivalence ratios. The study showed the ignition delay times of methanol to be in very good agreement with results from the literature (Fieweger et al., Comb. Flame 109 (1997) 599-619), whereas the other conditions had never been investigated before. The ignition delay time data were also in good agreement with modern detailed kinetics mechanisms such as the Aramco 2.0 model. The water time-history profiles were modeled using well-known literature mechanisms. Discrepancies were observed between these kinetics mechanisms, and poor predictions were observed for the lower temperatures investigated. Sensitivity and rate-of-

production analyses were performed using 3 literature mechanisms (namely, AramcoMech3.0, Princeton, and JetSurfII). Discrepancies were found among the models when predicting important reactions dominating the oxidation of methanol as well as the rate-of-production of H2O.

Ethanol Kinetics. Ethanol-based shock-tube experiments were performed over a similar range of conditions, mixtures, and measurements as described above for methanol. An additional set of ignition delay time experiments was performed for ethanol at higher pressures, namely between about 20 and 50 atm. Two mixtures chosen by the RCM kinetics community (spearheaded by Scott Goldsborough at ANL) were targeted for this special set of validation data. Several modern kinetics mechanisms agreed surprisingly well with these new data.

Isopropanol Kinetics. H2O formation during thermal decomposition of isopropanol was measured behind reflected shock waves at temperatures ranging from 1127 K to 1621 K at an average pressure of 1.42 atm using a laser absorption technique. Of the five modern chemical kinetics models used to compare the H2O time histories, the model from Li et al. 2019 showed the best overall agreement. Sensitivity and rate of production analyses using the Li et al. model (as well as those from AramcoMech 3.0, CRECK, and Togbe et al. 2011) showed unimolecular dehydration of isopropanol, iC3H7OH ⇌ H2O + C3H6 (R1), is nearly the sole reaction controlling H2O production at early times, allowing for an a priori measurement of the forward rate constant k1. The Arrhenius expression k1 (s-1) = 2.60×1013 exp(–31,120 K / T) was determined to represent best the data from this study. According to the models and previous experimental investigations, the pressure investigated is well within the high pressure limit (HPL) for this reaction. Additional, higher-pressure experiments also confirmed the HPL assumption. An uncertainty analysis was performed by varying secondary reactions within their uncertainties and examining their effect on the overall prediction, establishing an uncertainty within ±20% for all but the highest temperature cases which have a maximum uncertainty of ±35%. Experiments conducted with a radical trapper, toluene, showed little influence from radical chemistry, suggesting this estimated uncertainty is fairly conservative. Experimental data from Heyne et al. 2015 were found to be in good agreement with the rate measurements from this study and, therefore, a second Arrhenius expression, k1 (s-1) = 2.11×1013 exp(–30,820 K / T), was found to represent both datasets well. This second expression has a larger temperature range of 976 K to 1621 K. The present study provides the first high-temperature data collected for this reaction, adding to the limited data available for isopropanol in the literature.

Gasoline Surrogate Kinetics. Ignition delay times of a gasoline surrogate (iso-octane/toluene/n-heptane/1-hexene at 55/25/15/5% by liquid volume, proposed by McCormick/NREL) with high-level bio-blendstock-gasoline surrogate blends (50% and 85% biofuel by liquid volume of each ethanol and methyl acetate) were collected behind reflected shock waves. Post-reflected-shock temperatures ranged from 968 to 1361 K at pressures of 4, 10, 25, and 50 atm. Data were collected for real fuel-air mixtures at fuel lean and stoichiometric conditions (ϕ = 0.5, 1.0) with focus on the more-practical, fuel-lean conditions. Ignition delay times were measured from OH* chemiluminescence around 307 nm using an endwall diagnostic. Figure 14 shows some of the new data, namely for stoichiometric conditions and for 25 atm. The RON and MON of the surrogate were 90.3 and 84.7, respectively, which places it within the range of standard U.S. gasoline. Ethanol was chosen due to its wide use in flex-fuel vehicles and availability, while also providing an increased octane rating. Methyl acetate was chosen for its especially high octane rating to investigate the effect of an extreme case.

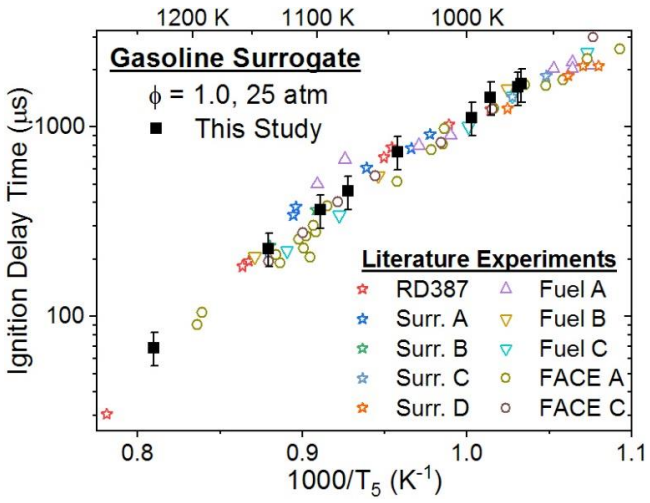

Figure 14. τ_{ign} data for the gasoline surrogate from this study at 25 atm and stoichiometric conditions compared to literature results pressure adjusted to 25 atm using the reported pressure exponent for each fuel.

To validate the gasoline surrogate, the data were compared to real gasoline (RD387) and several gasoline surrogate experiments from the literature. Using the wide range of pressures studied, the gasoline surrogate's pressure dependence was quantified to account for test-to-test variations using regression analysis. Similarly, a global correlation for gasoline and its surrogates was developed using all available data from the literature. Two modern chemical kinetics models targeting gasoline and its surrogates are compared to the ignition delay time measurements. Each model predicts ignition delay time values slower than those observed from experiment for virtually all mixtures, with better agreement occurring at higher temperatures and bioblendstock content. Significant disagreement between the models in the NTC region shape and location was also observed. These new high-pressure, high-bioblendstock concentration tests provide required chemical kinetic data for optimizing fuel and engine design.

Laminar Flame Speed Measurements

Laminar Flame speed measurements of a gasoline surrogate and mixtures of it with ethanol were conducted using a heated, constant-volume vessel. A spherical propagating flame was observed using a high-speed camera, and laminar flame speed was determined therefrom. The gasoline surrogate, which serves as the baseline for the current study, consisted of four components, namely, iso-octane, n-heptane, toluene, and 1-hexene. Different mixtures of the gasoline surrogate and ethanol were studied. They were governed by the ethanol percentage in the mixture. That is, E0, E30, E50, and E85 mixtures represent 0%, 30%, 50%, and 85% ethanol in the gasoline surrogate mixture by liquid volume, respectively. Several initial conditions were covered. Initial temperatures of 335, 359, and 408 K and initial pressures of 1 and 3 bar were investigated. The findings of this study were compared to results in the literature, which show good agreement for E0 but some deviation for the E30 blend. In general, the study showed an increase in laminar flame speed as the ethanol percentage increases in the mixture. Similarly, increasing the initial temperature with fixed ethanol percentage resulted in an increase in laminar flame speed, as expected. In contrast, increasing the initial pressure with fixed Ethanol percentage showed a decrease in laminar flame speed. Results were compared to an existing chemical kinetics model designed for ethanol and gasoline. Although agreement between the model and data is fair, new results show that some improvement to the kinetics model is needed. Figure 15 shows an example of laminar flame speed results

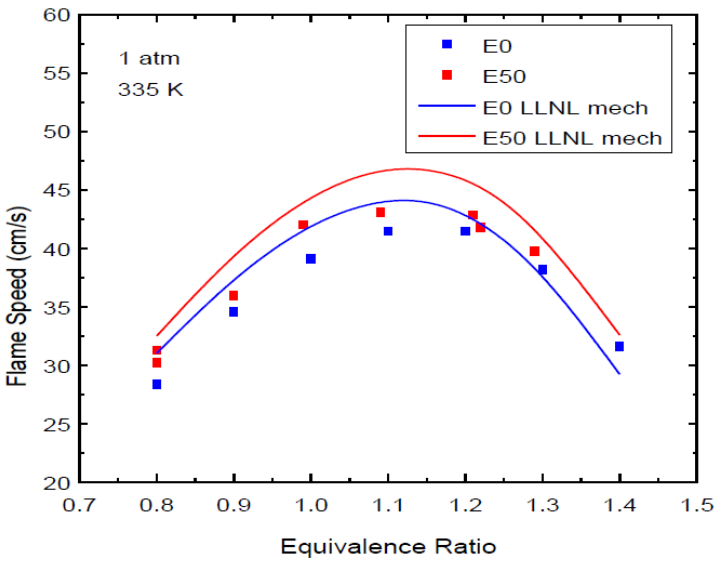

Figure 15. Laminar flame speed data for McCormick gasoline surrogate (E0) in comparison with new data taken for a blend with 50% ethanol (E50). Predictions using the LLNL gasoline model are also shown.

for a 50/50 (E50) blend in comparison with the TAMU gasoline data and the predictions of the LLNL chemical kinetics model.

Publication List

See References 7-11 and 31-33 in Section 7 (as reported by co-PI).

D. Reduced Mechanisms (co-PI T. Lu/UConn)

Summary

Reduced mechanisms for primary reference fuels blended with various biofuels are developed to support the effort of computational fluid dynamics (CFD) of the Co-Optima teams. The reduction was based on the detailed Lawrence Livermore National Laboratory (LLNL) mechanism [1], recently updated through the Co-Optima effort, that consists of 2878 species and 12839 elementary reactions. The reduction was based on a two-stage approach [2] with skeletal reduction being the first stage and quasi-steady state approximation (QSSA) based reduction being the second stage. The skeletal and reduced mechanisms have been extensively validated over a wide range of conditions relevant to engine applications, delivered to the Co-Optima teams, and employed in a variety of engine simulations.

Reduction method

The reduction method is based on the systematic approach reviewed in Ref. [2]. Specifically, the skeletal reduction is performed with the directed relation graph (DRG) and DRG-aided sensitivity analysis (DRGASA), and isomers with tightly correlated concentrations and similar reaction pathways are lumped to further reduced the number of transported species. The QSSA based reduction is based on the linearized quasi steady-state approximations (LQSSA) with the algebraic equations for QSSA analytically solved [3]. In addition, the stiff chemistry solver LSODES is implemented with sparse analytical Jacobian to speed up the iterative ignition delay time evaluations in the sensitivity analysis, such that substantial reduction in computational cost was achieved for the reduction process itself. Thirty-five sets of skeletal and reduced mechanisms were obtained, each for a different fuel blend and parameter range. The

selection of the pressure, temperature and equivalence ratio ranges are based on the target applications of each set of skeletal/reduced mechanisms as listed in the following section.

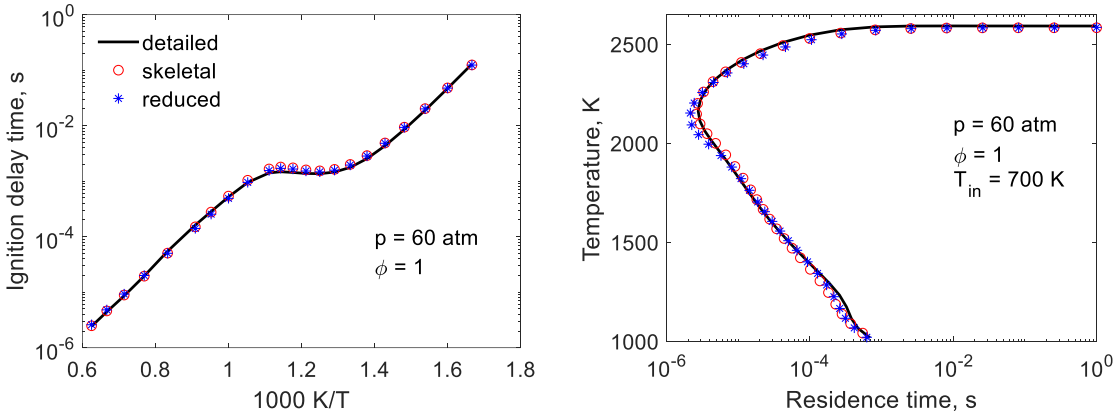

Figure 16. Selected ignition delay time and PSR validations for BOB-alk and air mixtures.

The skeletal and reduced mechanisms are extensively validated against the detailed mechanism for ignition delay, PSR extinction, and laminar flame speed that are relevant to both compression ignition and spark ignition engines, where examples are shown in Figure 16**.** Based on the validation results, these skeletal and reduced mechanisms are suitable for capturing auto-ignition at different initial temperatures, end-gas auto-ignition as well as flame propagation characteristics in both compression ignition and spark ignition engines.

List of skeletal/reduced mechanisms

The resulting skeletal/reduced mechanism sets are listed in Table 2, together with the range of pressure, equivalence ratio, and initial temperature for ignition, which is fixed to be 600K-1600K, including the negative temperature coefficient (NTC) regime, as well as the worst-case relative error tolerance for the reduction used for the reduction. The sampling range for perfectly stirred reactors (PSR), which is relevant to the high-temperature flame propagation and extinction behaviors share the same pressure and equivalence ratio ranges as those for auto-ignition and the inlet temperature for PSR is fixed to be 300K.

Table 2. List of skeletal/reduced mechanisms

Case No.	Fuels	Pressure range [atm]	Equivalence ratio	Initial temperature for ignition [K]	Relative Error Tolerance	Number of species (skeletal /reduced)
1	T-PRF-H-E with all biofuels	1-50	0.5-1.5	600-1600	0.4	317/208
2	T-PRF-H-E-DIB	1-50	0.5-1.5	600-1600	0.4	199/135
3	T-PRF-E	1-50	0.5-1.5	600-1600	0.4	189/126
4	T-PRF-DIB	1-50	0.5-1.5	600-1600	0.4	130/72
5	EXPERT	1-50	0.5-1.5	600-1600	0.4	113/64
6	BOBalk, BOBaro, BOBE30	1-50	0.5-1.5	600-1600	0.4	166
7	BOBalk	1-50	0.5-1.5	600-1600	0.4	109
8	BOBaro	1-50	0.5-1.5	600-1600	0.4	117
9	BOBE30	1-50	0.5-1.5	600-1600	0.4	112

10	TPRF-Anisole 0-30%	1-50	0.5-1.5	600-1600	0.4	129
11	TPRF-Anisole30%	1-50	0.5-1.5	600-1600	0.3	112
12	TPRF-isobutanol 0-30%	1-50	0.5-1.5	600-1600	0.4	131
13	PRF	1-50	0.5-1.5	600-1600	0.4	127/82
14	TPRF	1-50	0.5-1.5	600-1600	0.4	167/105
15	20% Anisole	1-50	0.5-1.5	600-1600	0.3	134
16	10% iso-butanol	1-50	0.5-1.5	600-1600	0.3	117
17	EXPERT	1-80	0.3-1.5	600-1600	0.3	129
18	T-PRF-DIB 0-50%	1-50	0.5-1.5	600-1600	0.3	171
19	EXPERT	1-80	0.3-1.5	600-1600	0.3	128
20	TPRF-E30	1-100	0.3-2.0	600-1600	0.2	149
21	TPRF-anisole 20%	1-80	0.8-1.2	600-1600	0.2	129
22	TPRF-isobut10%	1-80	0.8-1.2	600-1600	0.2	121
23	PRF	1-100	0.3-1.5	600-1600	0.3	178/127
24	3 BOBs	1-100	0.3-1.5	600-1600	0.3	211/148
25	TPRF	1-100	0.3-1.5	600-1600	0.3	259/193
26	BOBalk	1-100	0.3-1.5	600-1600	0.3	116/80
27	BOBaro	1-100	0.3-1.5	600-1600	0.3	140/105
28	BOBE30	1-100	0.3-1.5	600-1600	0.3	138/96
29	PRF90	1-100	0.2-0.6	600-1600	0.15	182
30	ethanol75%-nheptane25%	1-100	0.2-0.6	600-1600	0.2	130
31	tuluene75%-nheptane25%	1-100	0.2-0.6	600-1600	0.2	181
32	TPRF-DIB30%	1-80	0.8-1.2	600-1600	0.2	150
33	PRFE	1-100	0.3-1.5	600-1600	0.3	266/199
34	BOBO30	1-100	0.3-1.5	600-1600	0.3	181/101
35	BOBN30	1-100	0.3-1.5	600-1600	0.3	181/110

References

1. M. Mehl, K. Zhang, S. Wagnon, G. Kukkadapu, C.K. Westbrook, W.J. Pitz, Y. Zhang, H. Curran, M. Al Rachidi, N. Atef, M.S. Sarathy, A comprehensive detailed kinetic mechanism for the simulation of transportation fuels, in: 10th U.S. Natl. Combust. Meet., 2017: pp. 1–6.
2. T. Lu, C.K. Law, Toward accommodating realistic fuel chemistry in large-scale computations, Prog. Energy Combust. Sci. 35 (2009) 192–215.
3. T. Lu, C.K. Law, Systematic approach to obtain analytic solutions of quasi steady state species in reduced mechanisms, J. Phys. Chem. A. 110 (2006) 13202–13208.

Publication List

See References 12-17 in Section 7 (as reported by co-PI).

6. Conclusions

The following conclusions are found:

- Demonstrated viability of microliter fuel characterization and property prediction
- Confirmed existence of essential combustion modes up to 25 bars, which doubles peak pressure of comparable experiments documented in published work
- Documented the loss of an unstable combustion regime at diluted conditions, creating a new pathway for fuel testing at high pressures and prediction of octane rating
- Established framework for non-contact temperature measurements and machine-learning based classification of combustion regimes
- Demonstrated feasibility of piezo-electric fuel delivery and pathway for droplet-based measurements for surface tension, viscosity, vapor pressure and heat of vaporization
- Obtained high quality shock tube data for DOE reference blendstocks (methanol, ethanol, isopropanol and a 4-component gasoline surrogate)
- Produced a series of skeletal mechanisms that are used for predictive modeling

Results were documented and disseminated in 17 archival journal publications and 16 conference papers. Unpublished data are expected to result in several additional publications.

Follow-on efforts

Beyond CoOptima, applications of microliter fuel characterization and property prediction are highly relevant to sustainable aviation fuels, where funding opportunities are actively pursued.

Ongoing work on image processing is expected to produce substantial improvements of image quality of low-light exposures that are essential for diagnostics of weak flame chemiluminescence and pyrometry at low temperatures.

Acknowledgments

The PI's would like to thank the VTO leadership - Michael Berube, Gurpreet Singh, Kevin Stork, Ralph Nine, Michael Ursic, Michael Weismiller - as well as the DOE project mentor - Matthew McNenly - for their guidance and support.

7. List of Publications

Archival Journal Publications

1. N. Roohani, V. M. Sauer, and I. Schoegl, 2021. Effects of dilution and pressure on combustion characteristics within externally heated micro-tubes. *Proc. Combust. Inst.*, 38:6695–6702, doi:10.1016/j.proci.2020.06.090.

2. Schoegl, V. M. Sauer, and P. Sharma, 2019. Predicting combustion characteristics in externally heated microtubes. *Combust. Flame*, 204:33–48, doi:10.1016/j.combustflame.2019.02.029.

3. V. M. Sauer and I. Schoegl, 2019. Numerical assessment of uncertainty and dynamic range expansion of multispectral image-based pyrometry. *Measurement*, 145:820 – 832, doi:10.1016/j.measurement.2019.04.089.

4. W. Dang, M. Gurunadhan, W. Ard, I. Schoegl, and S. Menon, 2022. Droplet evaporation-based approach for microliter fuel property measurements. *Int. J. Thermophysics*, 43, doi:10.1007/s10765-022-02987-1.

5. W. Dang, M. Gurunadhan, I. Schoegl, and S. Menon, 2021. Temperature effects on droplet oscillation decay with application to fuel property measurement. *Atomizations and Sprays*, 31:1–23, doi:10.1615/AtomizSpr.2021039068.

6. W. Dang, W. Zhao, I. Schoegl, and S. Menon, 2020. A small-volume, high-throughput approach for surface tension and viscosity measurements of liquid fuels. *Meas. Sci. Technology*, 31:095301, doi:10.1088/1361-6501/ab8b23.

7. S. P. Cooper, C. M. Grégoire, D. J. Mohr, O. Mathieu, S. A. Alturaifi, and E. L. Petersen, 2021. An Experimental Kinetics Study of Isopropanol Pyrolysis and Oxidation behind Reflected Shock Waves. *Energies*, 14, doi.org/10.3390/en14206808

8. S. P. Cooper, O. Mathieu, I. Schoegl, and E. L. Petersen, 2020. High-pressure ignition delay time measurements of a four-component gasoline surrogate and its high-level blends with ethanol and methyl acetate. *Fuel*, 275:118016, doi:10.1016/j.fuel.2020.118016.

9. O. Mathieu, L. T. Pinzón, T. M. Atherley, C. R. Mulvihill, I. Schoegl, and E. L. Petersen, 2019. Experimental study of ethanol oxidation behind reflected shock waves: Ignition de- lay time and H2O laser-absorption measurements. *Combustion and Flame*, 208:313 – 326, doi:10.1016/j.combustflame.2019.07.005.

10. L. T. Pinzón, O. Mathieu, C. R. Mulvihill, I. Schoegl, and E. L. Petersen, 2019. Ignition delay time and H2O measurements during methanol oxidation behind reflected shock waves. *Combust. Flame*, 203:143–156, doi:10.1016/j.combustflame.2019.01.036.

11. L. T. Pinzón, O. Mathieu, C. R. Mulvihill, I. Schoegl, and E. L. Petersen, 2018. Ethanol pyrolysis kinetics using H2O time history measurements behind reflected shock waves. *Proc. Combust. Inst.*, 37:239–247, doi:10.1016/j.proci.2018.07.088.

12. Kim S., Scarcelli R., Wu Y., Rohwer J., Shah A., Rockstroh T., Lu T.F., "Simulations of Multi-Mode Combustion Regimes Realizable in a Gasoline Direct Injection Engine," *J. Energy Resour. Technol.*, 143(11) 112307 2021, doi:10.1115/1.4050589.

13. Kalvakala K.C., Pal P., Wu Y., Kukkadapu G., Kolodziej C., Gonzalez J.P., Waqas M.U., Lu T.F., Aggarwal S.K., and Som S., "Numerical analysis of fuel effects on advanced compression ignition using a cooperative fuel research engine computational fluid dynamics model," *J. Energy Resour. Technol.*, 143(10) 102304 2021, doi:10.1115/1.4050490.

14. Xu C., Pal P., Ren X., Som S., Sjoberg M., Van Dam N., Wu Y., Lu T.F., McNenly M., "Numerical investigation of fuel property effects on mixed-mode combustion in a spark-ignition engine," *J. Energy Resour. Technol.*, 143(4) 042306 2021, doi:10.1115/1.4048242.

15. Pal P., Kalvakala K., Wu Y., McNenly M., Lapointe S., Whitesides R., Lu T.F., Aggarwal S.K., Som S., "Numerical investigation of a central fuel property hypothesis under boosted spark-ignition conditions," *J. Energy Resour. Technol.*, 143(3) 032305 2021, doi:10.1115/1.4048995.

16. Pal, P., Kolodziej, C., Choi, S., Som S., Broatch A., Gomez-Soriano J., Wu Y., Lu T.F., See Y.C., "Development of a Virtual CFR Engine Model for Knocking Combustion Analysis," *SAE Int. J. Engines*, 11(6):2018, doi:10.4271/2018-01-0187.

17. Pal P., Wu Y., Lu T.F., Som S., See Y.C., Le Moine A., "Multi-dimensional CFD simulations of knocking combustion in a CFR engine", *J. Energy Resour. Technol.*, 140 (10) 102205 2018, doi:10.1115/1.4040063.

Conference Papers [1]

18. D. A. Akinpelu and I. Schoegl. Identification and Analysis of Chemical Reaction Modes. In *CSSCI Spring Meeting*, Detroit/MI, 2022.
19. D. A. Akinpelu and I. Schoegl. Towards a high-pressure microchannel reactor for fuel characterization. In *ASME 2021 Power Conference*, number POWER2021-64910, online, 2021. doi:10.1115/POWER2021-64910.
20. N. Roohani, V. M. Sauer, and I. Schoegl. Classification of microchannel flame regimes based on convolutional neural networks. In *ASME 2021 Power Conference*, number POWER2021-64437, online, 2021. doi:10.1115/POWER2021-64437.
21. D. A. Akinpelu and I. Schoegl. Effect of pressure and dilution level on the flame dynamics of CH_4/Air/N2 mixture in a heated microchannel. In *12th US Nat. Combustion Meeting*, online, 2021.
22. N. Roohani, V. M. Sauer, and I. Schoegl. Combustion characteristics of prfs within a pressurized externally heated micro-channel. In *12th US Nat. Combustion Meeting*, online, 2021.
23. D. A. Akinpelu and I. Schoegl. Numerical investigation of ignition characteristics of selected fuel blends in a micro reactor. In *11th US Nat. Combustion Meeting*, Pasadena/CA, 2019.
24. N. Roohani, V. M. Sauer, and I. Schoegl. Effects of dilution and pressure on combustion within externally heated microchannels. In *11th US Nat. Combustion Meeting*, Pasadena/CA, 2019.
25. V. M. Sauer and I. Schoegl. Quantifying the influence of camera sensor and optics on multispectral image-based thin filament pyrometry. In *11th US Nat. Combustion Meeting*, Pasadena/CA, 2019.
26. N. Roohani, V. Naralasetti, P. Sharma, V. M. Sauer, and I. Schoegl. Investigation of combus- tion characteristics of primary reference fuels in heated microchannels. In *WSSCI Spring Meeting*, Bend/OR, 2018.
27. V. M. Sauer, N. Roohani, and I. Schoegl. Toward calibration-free multi-band multi-wavelength pyrometry using low dynamic range CMOS cameras for combustion diagnostics. In *WSSCI Spring Meeting*, Bend/OR, 2018.
28. W. Dang, S. Menon, "Determination of heat of vaporization and vapor pressure by micro-liter fuel droplet vaporization", AIAA Propulsion and Energy Forum, August 24-26, 2020, New Orleans, LA, USA.
29. W. Dang, S. Menon, "Small-volume, High-throughput Techniques for Fuel Physical Property Measurements", AIAA Propulsion and Energy Forum, August 19-22, 2019, Indianapolis, IN, USA.
30. W. Dang, W. Zhao, S. Menon, "Evaporation of single droplets of multicomponent liquid fuel blends at elevated temperatures", ICLASS 2018: 14th International conference on liquid atomization & spray systems, July 22-26, 2018, Chicago, USA.
31. Y. M. Almarzooq, I. Schoegl, and E .L. Petersen. Laminar flame speed measurements of a gasoline surrogate and its mixtures with ethanol. In *12th US Nat. Combustion Meeting*, online, 2021.
32. T. M. Atherley, L. T. Pinzón, O. Mathieu, C. R. Mulvihill, I. Schoegl, and E. L. Petersen. Kinetics study of ethanol oxidation behind reflected shock waves: Ignition delay times, H2O measurements,

[1] Entries without DOI number are non-archival.

and detailed kinetics model comparisons. In *11th US Nat. Combustion Meeting*, Pasadena/CA, 2019.

33. O. Mathieu, L. T. Pinzón, T. M. Atherley, I. Schoegl, and E. L. Petersen. High-temperature non-homogeneous ignition of small alcohols behind reflected shock waves. In *27th Int. Colloq. Dyn. Explosions and Reactive Systems*, Beijing/CN, 2019.